Transmural Imaging of Ventricular Action Potentials and Post-Infarct Substrates in Swine Hearts

Linwei Wang[1], Fady Dawoud[2]

[1] Computing and Information Sciences, Rochester Institute of Technology, Rochester, NY, USA
[2] Johns Hopkins University School of Medicine, Baltimore, MD, USA

Abstract

Transmural electrophysiological imaging (TEPI) using surface measurements is an ill-posed problem that does not have a unique solution in its general unconstrained form. We previously developed and preliminarily validated a Bayesian approach to TEPI that incorporates physiological, spatiotemporal priors through probabilistic integration of dynamic electrophysiological models. The main contribution of this study is to generalize this method of TEPI, which previously considers data from body-surface electrocardiograms (ECG), to use inputs from electroanatomical voltage mapping (EAVM) on heart surfaces. Feasibility of this new application of TEPI is positively verified on two swine hearts. Furthermore, we involve multiple reference data in forms of in-vivo *EAVM and* ex-vivo *magnetic resonance imaging (MRI) of the post-infarct scar, allowing a detailed comparison of the three different modalities (EAVM, MRI & TEPI) for imaging/mapping post-infarct substrates. On the two swine models shared by* STACOM 2011 EP simulation challenge, *we are able to preliminarily demonstrate that, compared to the low-voltage surface scar area detected by EAVM, the 3D scar volume detected by TEPI is more consistent with scar volume delineated in MR images.*

1. Introduction

Characterization of post-infarct myocardial substrates is critical for defining preventative therapeutic strategy, such as catheter ablation of ventricular tachycardia (VT). The state-of-the-art ablation therapy is guided by electroanatomical voltage mapping (EAVM) of the patient's heart under sinus-rhythm. Acquired by point-to-point catheterized mapping on heart surfaces, EAVM often incurs excessive cost, patient discomfort/risk and prolonged mapping procedures [1]. Furthermore, EAVM provides a poor surface surrogate for deeply-situated myocardial substrates whose shapes often vary with the depth of the myocardium. Recent studies have reported evident mismatch between EVAM and delayed contrast-enhanced magnetic resonance imaging (DCE-MRI) in characterizing post-infarct substrates [1, 2]. Though still controversial, it is largely believed that EAVM cannot fully detect non-transmural infarct core or heterogeneous scar border [2]. Poor catheter contact and far-field recordings can also lead to false-positives on normal myocardium.

This gap in the standard of care calls for a transmural electrophysiological (EP) imaging modality that could reveal 3D subject-specific EP characteristics across the depth of the myocardium. This EP counterpart of traditional tomographic imaging could further compensate for the problems that structural imaging does not reveal functional conduction blocks in structurally normal myocardium, and that the routine use of MRI is not considered safe in ICD (implantable cardioverter-defibrillators) carriers.

However, to achieve the surface-to-volume transition of EP data involves an inverse problem notoriously known for its ill-posedness and the lack of a unique solution in its unconstrained form [3]. Starting with body-surface electrocardiograms (ECG), decades of research efforts arrived at surface solutions on the epicardium [4] or the ventricular surface [5] where information is not yet available along the depth of the myocardium. One of the first success in surface-to-volume transition focuses on the current density to infer EP activation isochrones and initiation sites [6].

We have previously developed [7, 8] and preliminarily verified [9, 10] a novel method of transmural EP imaging (TEPI) that combines body-surface ECG data and image-derived anatomical data of an individual to computationally reconstruct the *transmural action potentials* of the specific condition of a specific subject . The computed action potentials include not only the depolarization but also the repolarization activities, which are closely related to the vulnerability to arrhythmia and the location of arrhythmogenic substrates such as post-infarct scars [11].

In this paper, we initiate the generalization of TEPI to use heart-surface EAVM data that are available in EP laboratories, in particular the unipolar electrograms (EGM). This is motivated by the clinical potential of the EGM-based TEPI. Compared to the ECG-based TEPI, the EGM-based TEPI uses less *smeared* electrical data that are closer

to the heart and dose not need anatomical data of the torso. It thus sees more immediate application in standard EP study to provide transmural details that better guides therapy planning. We test the feasibility of this new potential application of EGM-TEPI on two swine hearts that were shared through *STACOM 2011 EP simulation challenge*.

Another focus of this study is to initiate the investigation on the relation between TEPI and the other two state-of-the-art modalities (EAVM and MRI) for post-infarct substrate imaging/mapping. We compare multiple state-of-the-art modalities including *in-vivo* EAVM and *ex-vivo* 3D MRI on each animal. This allows us to investigate the consistency and relation between the three different modalities (EAVM, MRI, and TEPI) for post-infarct substrate imaging/mapping, which could not be achieved in our earlier studies that involved only a single modality of reference data. We demonstrate preliminarily that TEPI-detected substrate is more consistent with MRI scar than EAVM is. It indicates that TEPI has the unique diagnostic potential to reveal functional and structural substrates of subject-specific abnormal EP activities that are of important therapeutic value but could be missed by EAVM or MR imaging alone.

2. Methods

The inverse problems of TEPI are not only intrinsically ill-posed but also suffer from the lack of a unique solution, *i.e.*, the spatial configuration of volume current sources cannot be determined uniquely from surface recordings [3]. To resolve this non-uniqueness,we incorporate two fundamental principles underlying our method of TEPI:

1. Incorporate physiological, spatiotemporal priors of action potentials using probabilistic integration of computational, dynamic EP models.
2. Combine this probabilistic priors with EGM data of uncertainty through Bayesian statistical regularization.

In the statistical setting, we view the transmural action potential $\mathbf{u}$ and the surface potential Φ as random fields. We seek the *maximum a posteriori* (MAP) estimate of $\mathbf{u_k}$ at each time instant k that maximizes the posterior density function of $\mathbf{u_k}$ given all the measurements available up to the time instant k, $\Phi_{1:k}$, where $k = 1, \cdots, T$ and T is the total number of data points of Φ in time.

$$\hat{\mathbf{u}}_k = \arg\max_{\mathbf{u_k}} \{ f(\mathbf{u_k}|\mathbf{\Phi_{1:k}}) \} \tag{1}$$

Combining the assumption of quasi-static bioelectrical field and the Markov property of action potentials, *Bayes rule* provides a pair of mutually recursive formulations to evaluate the posterior distribution $f(\mathbf{u_k}|\mathbf{\Phi_{1:k}})$:

$$f(\mathbf{u_k}|\mathbf{\Phi_{1:k-1}}) \propto \int_{\mathbf{u_{k-1}}} \underline{f(\mathbf{u_{k-1}}|\mathbf{\Phi_{1:k-1}})} f(\mathbf{u_k}|\mathbf{u_{k-1}}) \mathbf{du_{k-1}} \tag{2}$$

$$f(\mathbf{u_k}|\mathbf{\Phi_{1:k}}) \propto \underline{f(\mathbf{u_k}|\mathbf{\Phi_{1:k-1}})} f(\Phi_k|\mathbf{u_k}) \tag{3}$$

Prediction - model-based spatiotemporal priors: In equation (2), we first make a prediction of the distribution of $\mathbf{u_k}$ at the absence of data Φ_k, according to the estimate from the previous iteration $f(\mathbf{u_{k-1}}|\mathbf{\Phi_{1:k-1}})$ and incorporating the probabilistic prior knowledge of $\mathbf{u_k}$ reflected through $f(\mathbf{u_k}|\mathbf{u_{k-1}})$. Here we propose to incorporate a computational EP model $g(\mathbf{u})$ as a *blackbox* process behind $f(\mathbf{u_k}|\mathbf{u_{k-1}})$ to provide spatiotemporal priors, *i.e.*, the prediction (2) can be done by taking integrals of the priors predicted by $g(\mathbf{u})$ over the space of the previous estimate $\hat{\mathbf{u}}_{k-1}$. In this study, $g(\mathbf{u})$ is chosen to be the monodomain two-variable *Aliev-Panfilov* model [12], because it captures the macroscopic phenomenon of our targeted solutions (action potentials $\mathbf{u}$), without introducing infeasible computation or un-identifiable scales / variables in the inverse problem. Per the definition of prior knowledge, values of all the relevant model parameters are adopt *a priori* from the literature [12] rather than subject-specific.

Estimation - minimum mean square error estimate: After the Monte-Carlo simulation and integration of the *Aliev-Panfilov* model $g(\mathbf{u_{k-1}})$ over the space of $\hat{\mathbf{u}}_{k-1}$, we obtain the priors $f(\mathbf{u_k}|\phi_{\mathbf{1:k-1}})$ in equation (2). The posterior distribution $f(\mathbf{u_k}|\phi_{\mathbf{1:k}})$ can then be updated according to the Bayes rule in equation (3) and the MAP estimate can be generated. Here we take advantage of the widely-used Gaussian statistics so that the probabilistic density functions involved in equations (1 - 3) are completely described by their means and covariance matrices, and the posterior density function (3) and its MAP estimate (3) can be evaluated analytically through *minimum mean square error estimate*. For details of TEPI algorithm refer to [8].

3. Experiments

3.1. Experimental data processing

We consider data on two pre-clinical swine models, one healthy and the other with 5-week old chronic infarct, provided by the researchers in the *Sunnybrook Research Institute (Toronto, Canada)* and shared through *STACOM 2011 EP simulation challenge* [13]. For details of data acquisition and animal models, please refer to [13].

In-vivo EP data: Available to this study are endocardial and epicardial voltage maps recorded by CARTO-XP system (Biosense Webster, Inc., Diamond Bar, CA) during stable sinus rhythm. In current study we consider epicardial unipolar EGMs as inputs to the proposed EGM-TEPI. Temporal alignment of these EGM signals is done by the best matching QRS complexes in body surface lead III. Electrograms with correlation $\geq 90\%$ are selected as input signals (Fig 1 (a1)). Reference data include 1) infarct areas on the infarcted heart delineated from CARTO bipolar voltage maps (Fig 1 (a2)) using clinical cut-off threshold $< 1.5mV$; and 2) epicardial and endocardial isochrones of EP activation (Fig 1 (a3)).

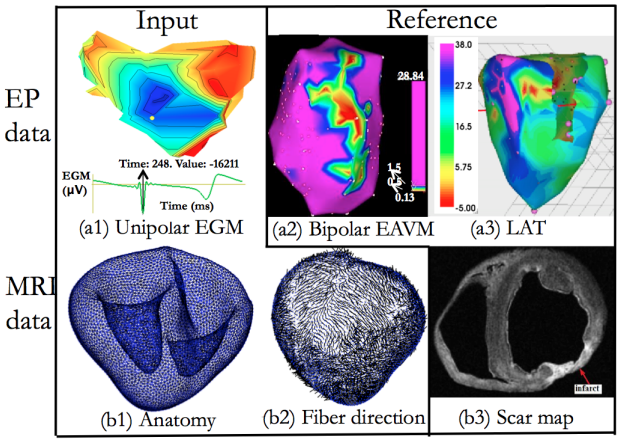

Figure 1. Input (a) and reference (b) data obtained from *in-vivo* electroanatomic mapping and *ex-vivo* MRI study. (c) Registration of CARTO points and MRI-derived data. Figures (a2) and (b3) are courtesy shared through STACOM 2011 EP simulation challenge website.

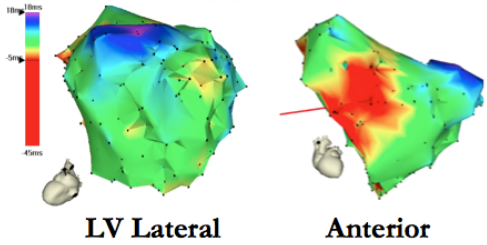

Figure 2. Epicardial activation isochrone maps acquired by CARTO-XP systems on the healthy porcine heart

Ex-vivo MRI data: 3D anatomical mesh (extracted from un-weighted MR images, Fig 1 (b1)) and fiber directions (estimated from diffusion weighted MR images, Fig 1 (b2)) were prepared and provided to this study by researchers at *Siemens Corporate Research (Princeton, NJ, USA)* and *INRIA Asclepios project (Sophia Antitpolis, France)*. Reference anatomical scar delineated from diffusion-weighted MR scans was provided by researchers from the *Sunnybrook Research Institute* (Fig 1 (b3)).

Registration of CARTO and imaging data: To integrate CARTO data and imaging data, rigid registration (rotation + translation) is first performed by an expert, in the custom research software via visual inspection of the ventricular shape and anatomical landmarks (primarily the scar areas) that are manually selected from CARTO points and the image-derived ventricular model (Fig 1 (c1)). After alignment, the input CARTO points are projected to the imaging surface via perpendicular projection (Fig 1 (c2)).

3.2. Results

Healthy Heart: Fig 2 shows activation isochrone maps measured by CARTO-XP systems on the healthy porcine heart. Ventricular excitations start at septal-apical region of LV endocardium and anterior-middle region of RV,

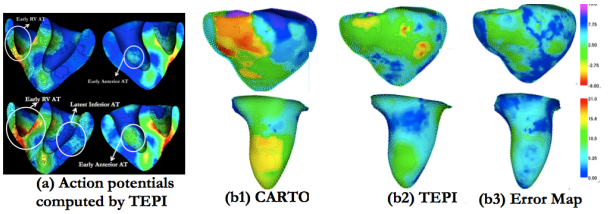

Figure 3. (a) Computed action potential at 14 and 19 ms after the onset of ventricular excitation (healthy heart). (b) Activation isochrone and error maps.

smoothly propagate through anterior walls and arrive at inferior-lateral LV at last. This RV-to-LV activation is different from *general* sinus-rhythm ventricular excitation.

Fig 3 (a) shows snapshots of the transmural EP computed by TEPI, which shows advanced RV activation and suppressed LV activation, particularly in the basal-anterior area. Fig 3 (b) shows the anterior views of the computed activation isochrone maps versus the CARTO data. The absolute error between the computed and CARTO activation map is $4.37 \pm 3.29ms$ on a $21ms$ span of total epicardial activation, and $7.03 \pm 4.29ms$ on a 29 ms span of total LV-endocardial activation.

Infarcted Heart: As shown earlier in Fig 1, the diseased porcine heart under study has a transmural anatomical scar that is centered at middle inferolateral LV, and extends longitudinally and circumferentially to the adjacent areas with decreasing percentage and transmurality.

Fig 4 (a) shows the transmural EP activation computed by TEPI, where LV excitation are suppressed and RV excitation are advanced, giving an LBBB-like pattern with sequential RV-to-LV, apex-to-base activation. Furthermore, there is a substantial delay at inferior-lateral LV, consistent to the locations of the anatomical scar enhanced in DW-MRI. Fig 4 (b) illustrate inferior-lateral views of epicardial and LV-endocardial activation isochrone, the average absolute errors versus CARTO measurements being $7.32 \pm 5.63ms$ on the epicardium on a span of $43ms$ total activation time, and $8.12 \pm 6.08ms$ on the LV endocardium on a span of $37ms$ total activation time.

Furthermore, using the activation time (AT) and action potential duration (APD) of the computed action potential, clustering analysis is applied to obtain the transmural localization of EP scar. Fig 5 illustrates the consistency between scars localized from the 3 modalities: EAVM (light blue), MRI (green), and TEPI (yellow). Overlaps are highlighted red. Quantitative evaluation of consistency between any two detected scar regions, S_1 and S_2, is defined by $r = (S_1 \cap S_2)/(S_1 \cup S_2)$.

Note in (a) the substantial mismatch of the scar detected by CARTO EAVM and MRI. The under-estimation of CARTO on the epicardium ((a) bottom) may indicate its inability to detect non-transmural scar border ($r = 21.25\%$), while its over-estimation on the endocardium

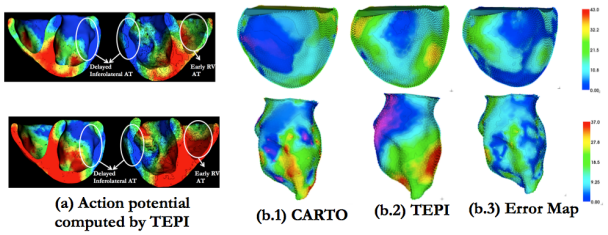

Figure 4. (a) Computed action potential at 29 and 34 ms after ventricular activation onset (infarcted heart). (b) Inferolateral view of epicardial (top) and LV-endocardial (bottomw) activation isochrone and error maps.

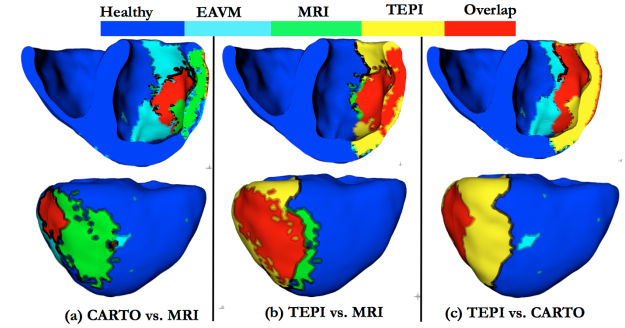

	(a) CARTO vs. MRI	(b) TEPI vs. MRI	(c) TEPI vs. CARTO
Epi	21.15%	64.65%	28.96%
Endo	25.29%	48.58%	29.71%
Transmural	N/A	59.53%	N/A

Figure 5. Superimposed substrates localized by CARTO EAVM, DW-MRI and TEPI. Top: transmural view. Bottom: Inferolateral epicardium.

((a) top) could be false-positives from poor catheter contact ($r = 25.29\%$). In comparison, the scar volume detected by TEPI is more consistent with MRI scar both on the epicardium ($r = 64.65\%$) and endocardium ($r = 48.58\%$). Its consistency with EAVM is also moderately higher than that between EAVM and MRI. Values of r between each of the 2 modalities are listed in Fig 5.

Conclusions: Our feasibility study demonstrates that, with *a priori* assumption of EP parameters available in literatures, EGM-TEPI is able to capture subject-specific transmural EP pattern with reasonable accuracy. Furthermore, the 3D scar volume detected by TEPI is more consistent with MRI scar volume than is the low-voltage area shown on heart-surface EAVM.It co-localizes with infarct core with high accuracy, and correlates with the outer border of scar that calls for future investigation.

Acknowledgements

The authors would like to thank Dr. Mihaela Pop, Dr. Graham Wright and their group (Sunnybrook Research Institute, Toronto, Canada) for the acquisition and sharing of the experimental data (EP-CARTO and DT-MRI data), Dr. Thomas Mansi (Siemens Corporate Research, Prince- ton, NJ, USA) and Dr. Maxime Sermesant (INRIA, Asclepios project, Sophia Antitpolis, France) for the mesh generation and fiber extraction for the heart models.

References

[1] Dickfeld T, Tian J, et al. MRI-guided ventricular tachycardia ablation: Integration of late gadolinium-enhanced 3d scar in patients with implantable cardioverter-defibrillators. Circ Arrhythm Electrophysiol 2011;4:172–184.

[2] Wijnmaalen AP, van der Geest RJ, et al. Head-to-head comparison of contrast-enhanced magnetic resonance imaging and electroanatomical voltage mapping to assess post-infarct scar characteristics in patients with ventricular tachycardias: Real-time image integration and reversed registration. European Heart Journal 2011;32:104–114.

[3] Plonsey R. Bioelectric phenonmena. New York: McGraw Hill, 1969.

[4] Rudy Y, Messinger-Rapport B. The inverse problem of electrocardiography: solutions in terms of epicardial potentials. Crit Rev Biomed Eng 1988;16:215–268.

[5] Huiskamp G, Greensite F. A new method for myocardial activation imaging. IEEE Trans Biomed Eng 1997;44(6):446.

[6] Liu Z, Liu C, He B. Noninvasive reconstruction of three-dimensional ventricular activation sequence from the inverse solution of distributed equivalent current density. IEEE Trans Medical Imaging 2006;25(10):1307–1318.

[7] Wang L, Zhang H, Liu H, Shi P. Imaging of 3D cardiac electrical activity: A model-based recovery framework. In Proc. MICCAI. 2006; 792–799.

[8] Wang L, Zhang H, Wong K, Liu H, Shi P. Physiological-model-constrained noninvasive reconstruction of volumetric myocardial transmembrane potentials. IEEE Trans Biomed Eng 2010;5(2):296–315.

[9] Wang L, Zhang H, Wong K, Liu H, Shi P. Noninvasive computational imaging of cardiac electrophysiology for 3-d infarct. IEEE Trans Biomed Eng 2011;58(4):1033–1043.

[10] Wang L, Dawoud F, et al. Mapping the transmural scar and activation for patients with ventricular arrhythmia. In Proc. Computing in Cardiology, volume 7085. 2011; 849–852.

[11] S. Ghosh JNS, Canham RM, Bowman TM, Zhang J, Rhee EK, Woodard PK, Rudy Y. Electrophysiologic substrate and intraventricular left ventricular dyssnchrony in nonischemic heart failure patients undergoing cardiac resynchronization therapy. Heart Rhythm 2011;8:692–699.

[12] Aliev RR, Panfilov AV. A simple two-variable model of cardiac excitation. Chaos Solitions Fractals 1996;7(3):293–301.

[13] Pop M, Sermesant M, et al. Forward approaches to computational electrophysiology using mri-based models and in-vivo carto mapping of swine hearts. In Proc of STACOM'11 workshop (Sept 2012, Toronto, CA) – Lecture Notes in Computer Science (Springer). 2012; 1–13.

Address for correspondence:

Linwei Wang
Rm 74-1075, 102 Lomb Memorial Dr., Rochester, NY 14534.
linwei.wang@rit.edu